Schubert, M., **Musolff, A.**, **Weiss, H.** (2018):
Influences of meteorological parameters on indoor radon concentrations (^{222}Rn) excluding the effects of forced ventilation and radon exhalation from soil and building materials
J. Environ. Radioact. **192** , 81 - 85

http://dx.doi.org/10.1016/j.jenvrad.2018.06.011

Influences of meteorological parameters on indoor radon concentrations (^{222}Rn) excluding the effects of forced ventilation and radon exhalation from soil and building materials

Michael Schubert[a], Andreas Musolff[a], Holger Weiss[a]

[a] UFZ - Helmholtz Centre for Environmental Research, Permoserstr. 15, 04318 Leipzig, Germany

Email: michael.schubert@ufz.de

Phone: 0049 341 235 1410

Abstract: Elevated indoor radon concentrations (^{222}Rn) in dwellings pose generally a potential health risk to the inhabitants. During the last decades a considerable number of studies discussed both the different sources of indoor radon and the drivers for diurnal and multi day variations of its concentration. While the potential sources are undisputed, controversial opinions exist regarding their individual relevance and regarding the driving influences that control varying radon indoor concentrations. These drivers include (i) cyclic forced ventilation of dwellings, (ii) the temporal variance of the radon exhalation from soil and building materials due to e.g. a varying moisture content and (iii) diurnal and multi day temperature and pressure patterns. The presented study discusses the influences of last-mentioned temporal meteorological parameters by effectively excluding the influences of forced ventilation and undefined radon exhalation. The results reveal the continuous variation of the indoor/outdoor pressure gradient as key driver for a constant "breathing" of any interior space, which affects the indoor radon concentration with both diurnal and multi day patterns. The diurnally recurring variation of the pressure gradient is predominantly triggered by the day/night cycle of the indoor temperature that is associated with an expansion/contraction of the indoor air volume. Multi day patterns, on the other hand, are mainly due to periods of negative air pressure indoors that is triggered by periods of elevated wind speeds as a result of Bernoulli's principle.

Influences of meteorological parameters on indoor radon concentrations (^{222}Rn) excluding the effects of forced ventilation and radon exhalation from soil and building materials

1 Introduction

Elevated concentrations of the naturally occurring radioisotope ^{222}Rn (hereafter referred to as "radon") in residential indoor air have been increasingly recognized as potential health risk during the last decades (e.g. WHO, 2009). As a consequence a considerable number of large-scale indoor radon surveys have been conducted in several European countries. Major purpose of these surveys was to establish national reference levels and/or threshold values that can serve as basis for the setup of action plans that aim at limiting the indoor radon exposure to humans (e.g. European Council, 2014; Tollefsen et al., 2014; EEA, 2013).

The studies revealed that the indoor radon concentration in residential homes is governed by ventilation habits, meteorological parameters, individual building characteristics, and by the geological and physical conditions of the soil where radon is constantly being produced. Since the latter is (besides forced ventilation) a particularly influential factor, the necessity of the local enforcement of radon related legislation is mainly determined by the geological and geographical setting of the area in question. The related influential parameters of the soil are often summarized as its "radon potential" (e.g. Chen and Ford, 2017; Schmid and Wiegand, 1998). Its large-scale spatial mapping is a key tool for radon related risk assessments of residential areas and allows furthermore the optimization of small-scale radon surveys that aim at preventing or mitigating radon exposure to humans (Ciotoli et al., 2017).

However, radon accumulation in dwellings is not only controlled by radon exhalation from the subsoil or building materials and by forced ventilation. Strongly influential are also the local time-variant meteorological conditions (e.g. Cinelli et al., 2011; Yarmoshenko et al., 2016). Related time-variant influential parameters include soil moisture, soil and air temperature incl. the associated gradients, wind speed, and air pressure (e.g. Schubert and

Schulz, 2002). Studies that focused on diurnal variations of indoor radon concentrations have shown that they are generally higher in the early morning hours and lower in the early afternoon (e.g. Murty et al., 2010; Karunakara et al., 2005). While some authors associate this temporal pattern primarily to the increased forced ventilation of the rooms during the daytime (e.g. Vaupotic et al., 2012), others suggest the generally observed diurnal variations of wind speed, air pressure and/or temperature as interrelated key drivers (Goglack and Beck, 1980; Porstendörfer et al., 1991; Porstendörfer, 1994; Schubert and Schulz, 2002).

Most recent studies that focus on diurnal changes in indoor radon concentration discuss the combined impact of (i) individual ventilation habits, (ii) building characteristics, (iii) radon exhalation from soil and building material and (iv) meteorological influences. However, approaches that allow disentangling the individual contributions of these impacts are scarce. In the presented study we used an experimental setup that allows focusing exclusively on the meteorological influences by effectively eliminating the influence of both forced ventilation and undefined radon exhalation.

Continuous time series of radon concentration, temperature, air pressure and wind speed were recorded over a two month period inside and outside a closed (but not completely air-tight) container that was exposed to meteorological influences. The container was equipped with a defined radon point source. No other potential radon source (subsoil, building material) was present within the container. Hence, the approach resulted in indoor radon time series that were unaffected by both soil or building characteristics and ventilation habits. The results allowed thus the individual evaluation of the impact of varying indoor/outdoor gradients of meteorological parameters.

2 Materials and methods

2.1 Determination of radon exhalation rate

A piece of high grade uranium ore (pitchblende) from the vein-type deposit Niederschlema-Alberoda, Germany, was used as radon point source. For determination of its radon exhalation rate measurements were carried out under laboratory conditions applying a mobile radon-in-air monitor (AlphaGuard, Saphymo). For the measurements the source was placed in a radon-tight stainless steel box (volume 0.2 m^3) that was equipped with an inlet and an outlet port. After placing the source in the box the box was closed and sealed. Subsequently the enclosed air volume was pumped in a closed loop through box and radon monitor by means of a radon-tight gas pump (AlphaPump, Saphymo). Both detector and pump were placed on the lid of the steel box, which allowed keeping the (also radon-tight) connecting tubing (Tygon, Saint-Gobain) as short as possible (in total ca. 50 cm). The radon inventory of the air volume (I_{Rn}; [Bq]) was recorded continuously as time series in 10 min counting intervals. The total volume of circulating air was 0.2005 m^3. The pump rate was kept constant at 1000 cm^3/min. The experiment was carried out twice in order to improve the statistical reliability of the result. Each measurement started with a radon background concentration of 25 Bq/m^3, which equals a radon background inventory of the closed system of I_{Rn} = 5 Bq.

Continuous radon exhalation from the radon point source resulted in a gradual increase of I_{Rn} within the closed system. The slope of that increase started with a virtually linear rise that flattened out with time and gradually approached a steady state plateau. The calculation of the radon exhalation rate of the radon point source was made in two independent ways, (i) based on the virtually linear slope of the I_{Rn} increase that was recorded during the first three hours and (ii) based on the final steady state inventory of the circulating air volume.

2.2 Container measurements

For investigation of the influences of varying meteorological parameters on the indoor radon concentration excluding the effects of forced ventilation and radon exhalation from soil and building materials a 33.2 m^3 (5.90 x 2.36 x 2.38 m) steel container was placed outdoors where it was exposed to wind, temperature and air pressure. Within the container the radon point source was placed in front of a desk ventilator, which kept the container indoor air continuously in slight motion. Radon concentrations, air temperatures and air pressures were measured both inside and outside the container as continuous time series over a period of two months by means of two mobile AlphaGuard radon monitors. Both monitors were run simultaneously set to a 10 min counting cycle. Additionally the pressure gradient between inside and outside of the container was recorded by means of a low-level pressure difference monitor (Multi Sensor Unit, Genitron). Furthermore the outside wind speed was recorded using a mobile weather station (Kestrel® 4500). Missing wind speed values that resulted from short-term power outages of the weather station were filled with equivalent data from an external nearby station. A bias-correction was applied to these external data using a linear relation between external smoothed measurements as predictor and local smoothed measurements as response ($R^2 = 0.48$).

For radon measurements both indoor and outside air were pumped into the respective AlphaGuard detection chambers at a rate of 0.3 L/min. The outside radon monitor was placed on the roof of the container sheltered by a tarpaulin. The indoor radon monitor was placed in the center of the container. The doors of the container were kept shut all the time. Still, a small ventilation hole in the container wall (2 above the container floor) was kept open to allow limited air exchange with the outside. The hole was ca. 3 cm in diameter and covered by a screen plate that sheltered it from the direct impact of wind gusts. The container was completely purged with outside air before the experiment was started. For the evaluation of the final indoor and outdoor Rn time-series, smoothing by running mean and correlation analysis (Pearson's correlation) was used.

3 Results and discussion

3.1 Determination of radon exhalation rate

Two completely independent datasets were used for calibration of the radon point source (each with $n = 2$): the initial I_{Rn} slope that developed over the first three hours of the measurement and the final I_{Rn} equilibrium that was reached after about three weeks and was confirmed with a fitted function (Fig. 1). In the initial stage of each experiment the I_{Rn} vs.

time slope represented the radon exhalation rate of the point source directly (F_{slope} [Bq/s]). The final steady state phase, on the other hand, allowed calculating the radon exhalation rate within the steel box that is needed for maintaining the steady state concentration (F_{eq} [Bq/s]). The F_{slope} data revealed a radon exhalation rate of the point source of 0.26 Bq/s with a high statistical reliability ($R^2 = 0.99$; Fig. 1A). The F_{eq} dataset revealed a steady state radon inventory of 114 kBq (Fig. 2B), which implies a constant support by a radon exhalation of 0.24 Bq/s, thus agreeing with the value revealed by F_{slope}. Since undesired radon escape from the closed system during the three weeks of the experiment cannot be ruled out completely the radon exhalation from the point source was defined to be 0.26 Bq/s as revealed by the initial slope.

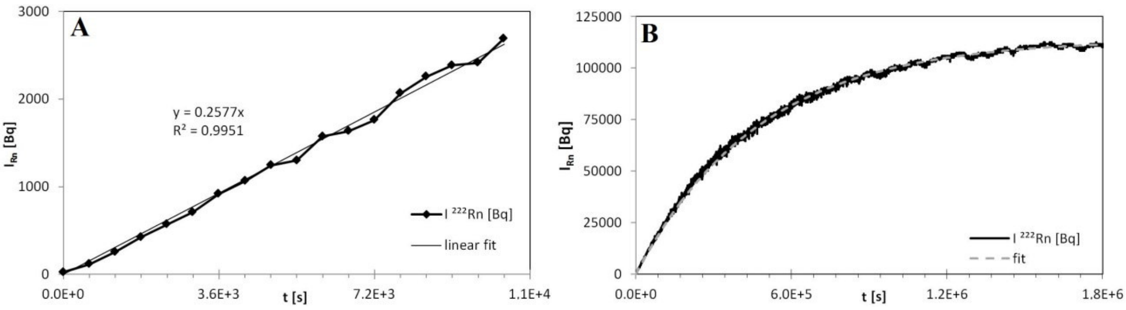

Fig. 1: Source calibration datasets "radon inventory vs. time" revealing an exhalation rate of $F_{slope} = 0.26$ Bq/s based on the initial slope (1A) and an exhalation rate of $F_{eq} = 0.24$ Bq/s based on the steady state inventory ($I_{Rn} = 114$ kBq; 1B)

3.2 Container measurements

3.2.1 Initial slope

All field data was recorded as time series in 10 min intervals. After starting the measurement it took about six days to reach steady state conditions within the container, i.e. an indoor radon concentration (of about 1.8 kBq/m³) that is in equilibrium with the exhalation rate of the point source under the given conditions (i.e. air volume and the limited air exchange rate of the container).

The slope of the gradually rising indoor radon inventory during the initial seven hours of the experiment is displayed in Fig. 2. It reveals a radon exhalation rate of the point source of 0.38 Bq/s. This exhalation rate is 0.12 Bq/s higher than the one calculated based on the data from the source calibration experiment under laboratory conditions but is still in the same range. The slightly higher exhalation rate that was detected in the container might be due to an elevated moisture content of the radon source due to the given outside conditions in the container (Stranden et al., 1984). Additionally it has to be noted that the coefficient of determination of the linear regression of the applied seven hours' time series is lower than the associated value of the laboratory experiment, indicating a lower statistical reliability of the resulting value. This higher variability of the radon data becomes obvious in the rather unsteady plot shown in Fig. 2 (if compared to Fig. 1). It is a result of the low concentrations in the initial stage of the container experiment.

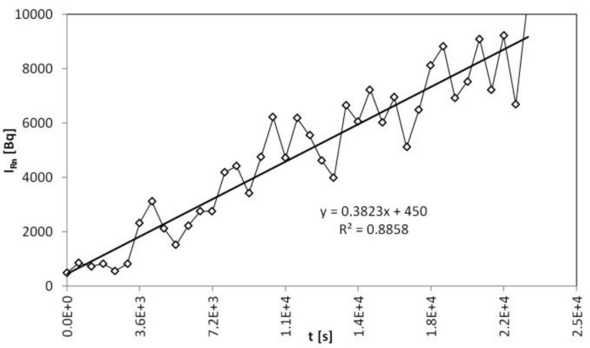

Fig. 2: Dataset "radon inventory vs. time" revealing an initial slope of 0.34 Bq/s

3.2.2 Diurnal variations

Both the recorded indoor and outdoor radon time series show consistent daily variations. Fig. 3 displays the individual diurnal patterns averaged over the complete runtime of the experiment (excluding the increase indoors over the initial six days). The noise is smoothed out by using a running mean of twelve 10 min steps. Both plots show the same general pattern: elevated concentrations in the morning and lower concentrations in the afternoon.

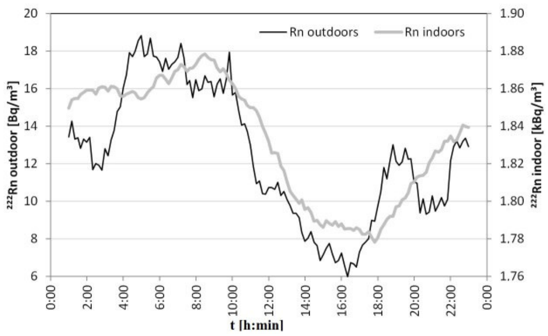

Fig. 3: Diurnal radon patterns averaged over the complete two months runtime

A comparable pattern has been reported for radon concentrations measured directly at the soil surface by Schubert and Schulz (2002). The authors explained this characteristic diurnal pattern with the periodically inverting temperature gradient in the top soil layer, which governs the magnitude of the contribution of convective soil gas migration to the overall radon exhalation from the soil pore space (including both advection and diffusion). They argued that the cooler temperature of the air compared to the soil temperature during the early morning is triggering convective radon degassing. During the afternoon, on the other hand, the temperature gradient is inversed thus hampering a “thermal breathing” of the soil and obstructing radon exhalation.

The average diurnal concentration pattern that was measured outside the container during the experiment could be explained with this temperature gradient triggered process discussed by Schubert and Schulz (2002). However, the diurnal radon concentration pattern recorded within the container must be caused by different drivers. The outside temperature was always cooler than the inside temperature of the container (on average by 3.4 °C), which implies that no cyclic inversion of the temperature gradient between outside and container interior took place. Temperature-triggered ventilation of the container is hence not driven by a periodical “thermal sealing” as discussed by Schubert and Schulz (2002) but rather by the absolute indoor temperature. This diurnal temperature pattern varied between about 9 °C in the morning and about 17 °C in the late afternoon (thus covering a temperature range of 8 K) and plotted inversely to the pattern of the indoor radon concentration (Fig. 4).

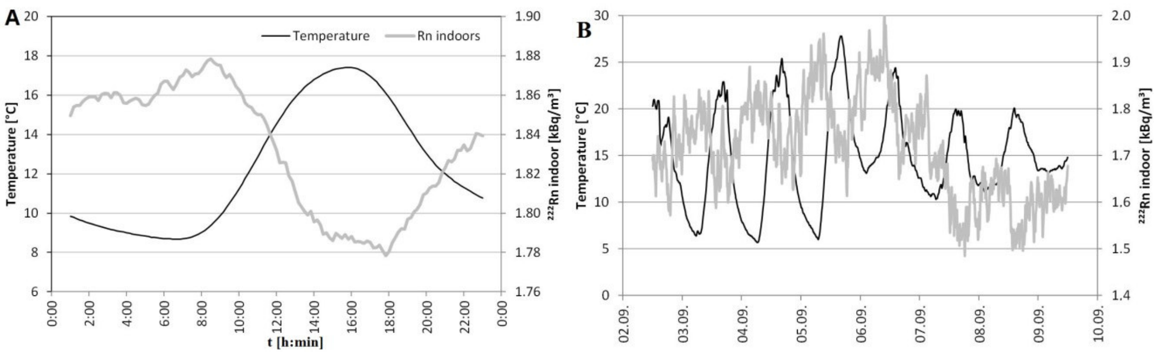

Fig. 4 A: Diurnal indoor radon and temperature patterns averaged over the complete two months runtime; 4B: Exemplary unprocessed 1 week time series of indoor radon and temperature

The periodical up and down of the indoor temperature results in a periodical expansion and contraction of the indoor air volume. Due to the ventilation hole in the container wall the expansion during the day (warmer) doesn’t result in buildup of a higher inside pressure but in radon “rich” air leaving the container thus leveling out the pressure gradient. On the other hand, at night (cooler) the air contraction doesn’t result in in buildup of a lower inside pressure but in radon “poor” outside air being sucked into the container thus again leveling out the pressure gradient. This process results in the recorded diurnally varying steady state.

Any air volume expands by 0.367 % per Kelvin. That means in our case that the 32 m³ air volume within the container expanded periodically between morning and late afternoon by ca. 3 % (corresponding to a ΔT of 8 K), thus reducing the radon concentration within this “heating up” period periodically by ca. 0.06 kBq/m³. That would theoretically result in an indoor radon concentration of ca. 1.81 kBq/m³ at the end of this expansion phase (i.e. at around 16:00 pm), a value that comes close to the detected 1.78 kBq/m³.

Still, it has to be pointed out, that the cyclical expansion and contraction of the indoor air volume due to the diurnally varying indoor temperature is not the only driver that triggers the “breathing” of the container, which in turn reduces the indoor radon concentration periodically. As displayed exemplarily in Fig. 5 the wind speed does also show an apparent day/night cycle. Highest wind speeds appear generally at about noon and in the early afternoon; the lowest ones around midnight. This diurnal wind speed pattern has to be considered as additional driver for the "breathing" since the wind induces lower pressure on the surface of the container due to Bernoulli’s principle (an increase in the speed of any fluid occurs simultaneously with a decrease in pressure). This negative pressure in the container adds to the “thermal breathing” discussed above.

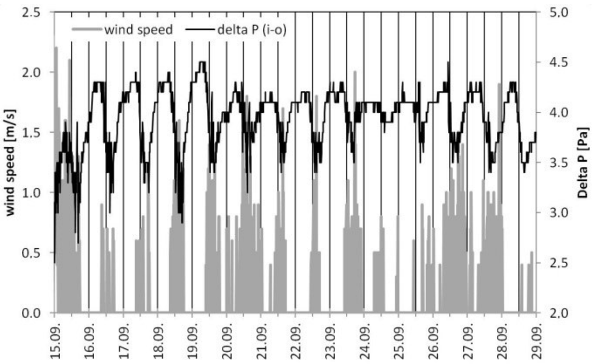

Fig. 5: Exemplary time series (2 weeks) of wind speed and indoor-outdoor pressure gradient

Schubert and Schulz (2002) argued that low wind speeds are minimizing air turbulences close to the ground thus adding to the increase of the radon concentration at the soil/air interface at night driven by soil exhalation. Goglack and Beck (1980) assumed that this rather stable nightly atmospheric stratification, which hampers radon dilution close to the ground, has even a stronger impact than the diurnally varying radon exhalation rate. Such atmospheric stratification might be responsible for the measured outside radon pattern recorded during our container experiment. However, it cannot be used for explaining the much more distinct indoor radon pattern. The interior of the container was not influenced by any variable air turbulences since the container allowed only very limited exchange with the outside air. The recorded diurnal indoor radon pattern must thus first and foremost be interpreted as a result of the breathing of the container triggered by temperature and wind speed as discussed above.

3.2.3 Multi day variations

The variable inside/outside pressure gradient that is triggered by changing wind speeds (i.e. as a result of Bernoulli's principle) becomes evident not only in the diurnal patterns discussed above and illustrated in Fig. 5 but reflects even more evidently in the multi day variations of the indoor radon concentration. Figs. 6 and 7 display the wind speed over the complete two months runtime of the experiment along with the simultaneously recorded inside/outside pressure gradient and the radon indoor concentration, respectively. The displayed time-series indicate the strong interconnection of wind speed, pressure gradient and indoor radon concentration evidently. This can be underpinned by a good correlation of mean daily pressure gradient delta P with mean daily wind speed (r = -0.65). Large pressure gradients, represented by large daily ranges of delta P, result in strong negative concentration changes (Fig. 7b). High wind speeds trigger negative pressure in the container leading to reduced radon concentrations.

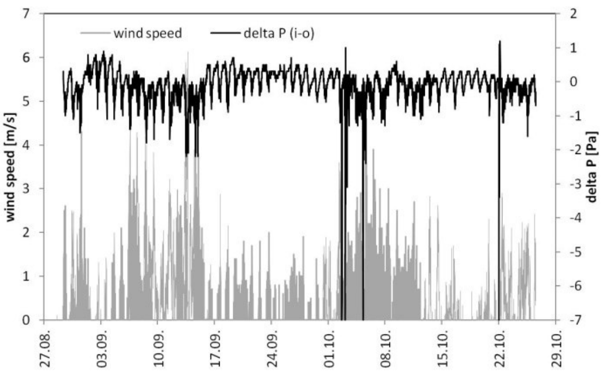

Fig. 6: Wind speed and indoor/outdoor pressure difference time series over the complete runtime of the experiment

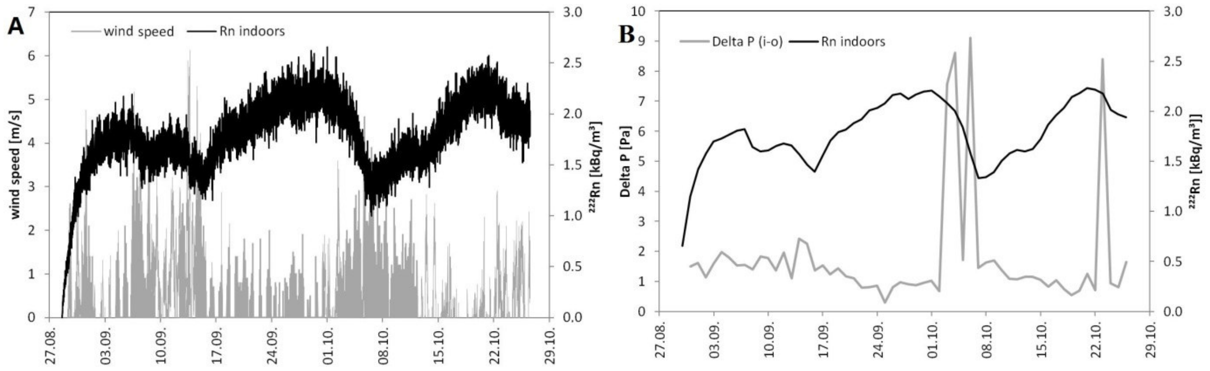

Fig. 7: Indoor radon concentrations (10 min values as recorded) and (7A) wind speed time series (10 min values as recorded) and (7B) pressure gradients (averaged day values) over the complete runtime of the experiment. Increased negative pressure indoors that is triggered by a higher wind speed results in a pressure induced "breathing" of the container.

4 Conclusions

The recorded datasets allow an evaluation of the dependence of the indoor radon concentration on meteorological parameters excluding the influence of forced ventilation and radon exhalation from soil and building materials. Varying indoor/outdoor air pressure differences were revealed as key driver for a continuous indoor/outdoor air exchange and thus for the variation of the indoor radon concentration. This "breathing" of the container was revealed to occur both with diurnal and multi day patterns. The diurnal variation of the indoor radon concentration was predominantly triggered by the diurnally changing indoor temperature and the associated expansion/contraction of the indoor air volume. Adding to this thermal breathing were diurnally recurring periods of low pressure within the container triggered by an elevated wind speed that generally arises during early afternoons. This influence is founded on Bernoulli's principle. Besides its diurnally changing impact the latter effect resulted also in multi day breathing patterns associated to multi day periods of stronger winds. Thus it can be concluded that while the thermal breathing was identified as major cause of the diurnal variation of the indoor radon concentration, multi day radon variations seem mainly be a result of multi day wind speed patterns.

REFERENCES

Chen, J., Ford, K.L., 2017. A study on the correlation between soil radon potential and average indoor radon potential in Canadian cities. J. Envir. Radioac. 166 (1), 152-156.

Cinelli, G., Tondeur, F., Dehandschutter, B., 2011. Development of an indoor radon risk map of the Walloon region of Belgium, integrating geological information. Environ. Earth Sci. 62 (4), 809-819.

Ciotoli, G., Voltaggio, M., Tuccimei, P., Soligo, M., Pasculli, A., Beaubien, S.E., Bigi S., 2017. Geographically weighted regression and geostatistical techniques to construct the geogenic radon potential map of the Lazio region: A methodological proposal for the European Atlas of Natural Radiation. J. Envir. Radioac. 166 (2), 355-375.

EEA - European Environment Agency, 2013. European Indoor Radon map, Last modified 11 Jun 2013. ww.eea.europa.eu/data-and-maps/figures/european-indoor-radon-map-december-2011

European Council, 2014. Council Directive 2013/59/Euratom of 5 December 2013 laying down basic safety standards for protection against the dangers arising from exposure to ionising radiation, and repealing Directives 89/618/Euratom, 90/641/Euratom, 96/29/Euratom, 97/43/Euratom and 2003/122/Euratom. Off. J. Eur. Union 57 (L13), 1–73 (Available at http://eur-lex.europa.eu/JOHtml.do?uri=OJ:L:2014:013:SOM:EN:HTML).

Gogolak, C.V., Beck, H. L., 1980. Diurnal variation of radon daughter concentrations in the lower atmosphere. In: Natural Radiation Environment III, Vol. 1, Ed. Gesell, T.F. and Lowder, W.M., U.S. Department of Energy, Washington D.C. CONF-780422, 259-280.

Karunakara, N., Somashekarappa, H.M., Rajashekara, K.M., Siddappa, K., 2005. Indoor and outdoor radon levels and their diurnal variations in the environs of southwest coast of India. International Congress Series 1276, 341-343.

Murty, V.R.K., King, J.G., Karunakara, N., Raju, V.C.C., 2010. Indoor and outdoor radon levels and its diurnal variations in Botswana. Nucl. Instr. Meth. Phys. Res. A 619 (1–3), 446-448

Porstendörfer, J., Butterweck, G., Reineking, A., 1994. Daily Variations of the Radon Concentration Indoors and Outdoors and the Influence of Meteorological Parameters. Health Phys. 67 (3), 283 – 287.

Porstendörfer, J., Butterweck, G., Reineking A., 1991. Diurnal variation of the concentrations of radon and its short-lived daughters in the atmosphere near the ground. Atmos. Environ. A. General Topics 25 (3-4), 709-713.

Schmid, S., Wiegand, J., 1998. The influence of traffic vibrations on the radon potential. Health Physics 74, 231-236.

Schubert, M., Schulz, H., 2002. Diurnal radon variations in the upper soil layers and at the soil-air interface related to meteorological parameters. Health Physics 83, 91-96.

Stranden, E., Kolstad, A.K., Lind, B., 1984. Radon exhalation: moisture and temperature dependence. Health Physics 47, 480-484.

Tollefsen, T., Cinelli, G., Bossew, P., Gruber, V., De Cort M., 2014. From the European indoor radon map towards an atlas of natural radiation. Radiat. Prot. Dosimetry 162 (1-2), 129-134.

Vaupotic, J., Bezek, M., Kavasi, N., Ishikawa, T., Yonehara, H., Tokonami, S., 2012. Radon and thoron doses in kindergardens and elementary schools. Radiat. Prot. Dosimetry 152 (1–3), 247-252.

WHO, 2009. WHO Handbook on Indoor Radon: A Public Health Perspective. World Health Organization (978 92 4 154,767 3), Available at http://www.who.int/ionizing_radiation/env/radon/en/index1.html.

Yarmoshenko, I., Vasilyev, A., Malinovsky, G., Bossew, P., Žunić, Z.S., Onischenko, A., Zhukovsky, M., 2016. Variance of indoor radon concentration: Major influencing factors. Sci. Total. Environ. 541, 155-160.

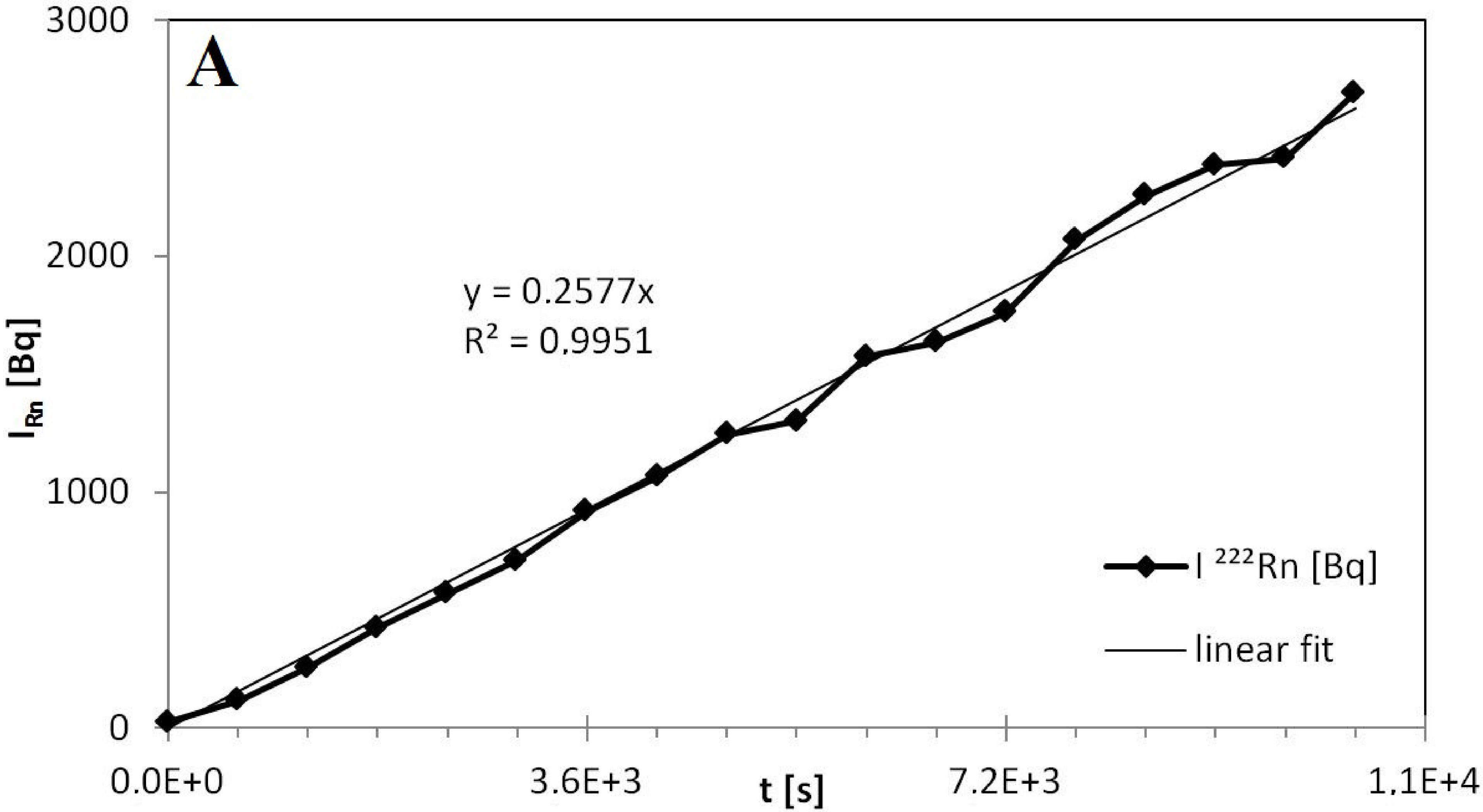

A
3000
2000
1000
0
I_{Rn} [Bq]
y = 0.2577x
R² = 0.9951
I ²²²Rn [Bq]
linear fit
0.0E+0
3.6E+3
7.2E+3
1.1E+4
t [s]

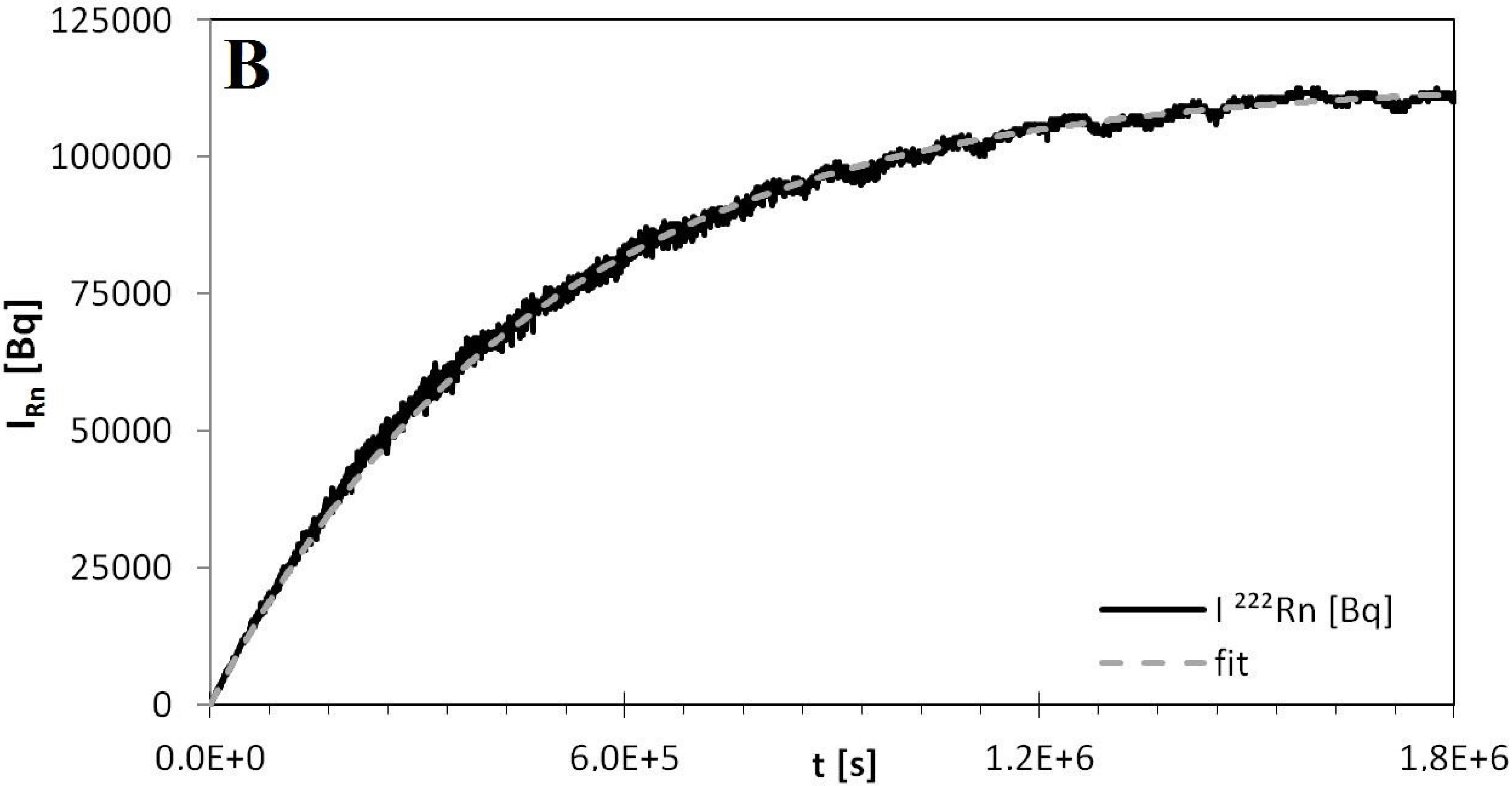

B
125000
100000
75000
50000
25000
0
I_{Rn} [Bq]
I ^{222}Rn [Bq]
fit
0.0E+0
6,0E+5
1.2E+6
1,8E+6
t [s]

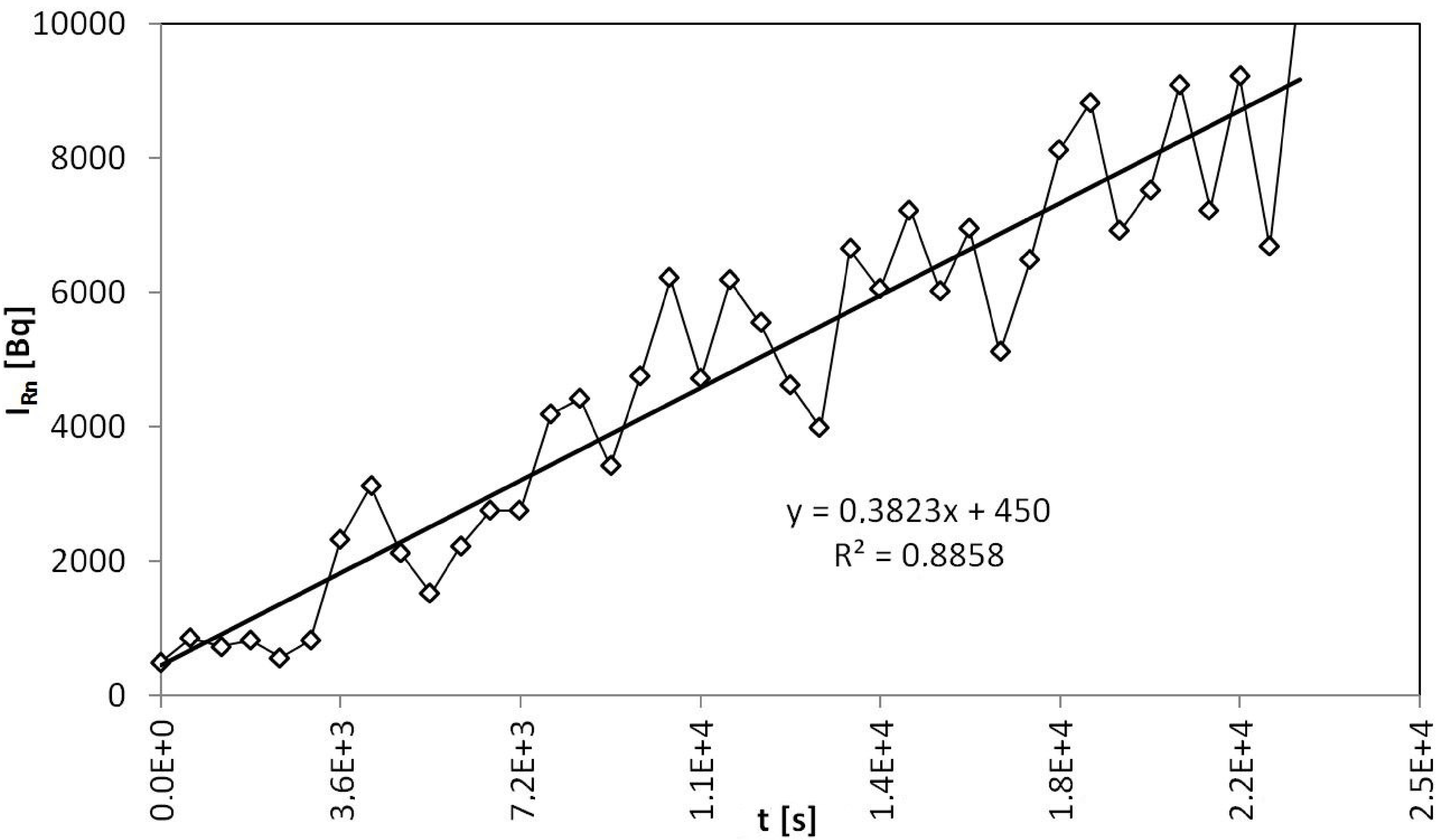

10000
8000
6000
4000
2000
0
I_{Rn} [Bq]
y = 0.3823x + 450
R^2 = 0.8858
0.0E+0
3.6E+3
7.2E+3
1.1E+4
1.4E+4
1.8E+4
2.2E+4
2.5E+4
t [s]

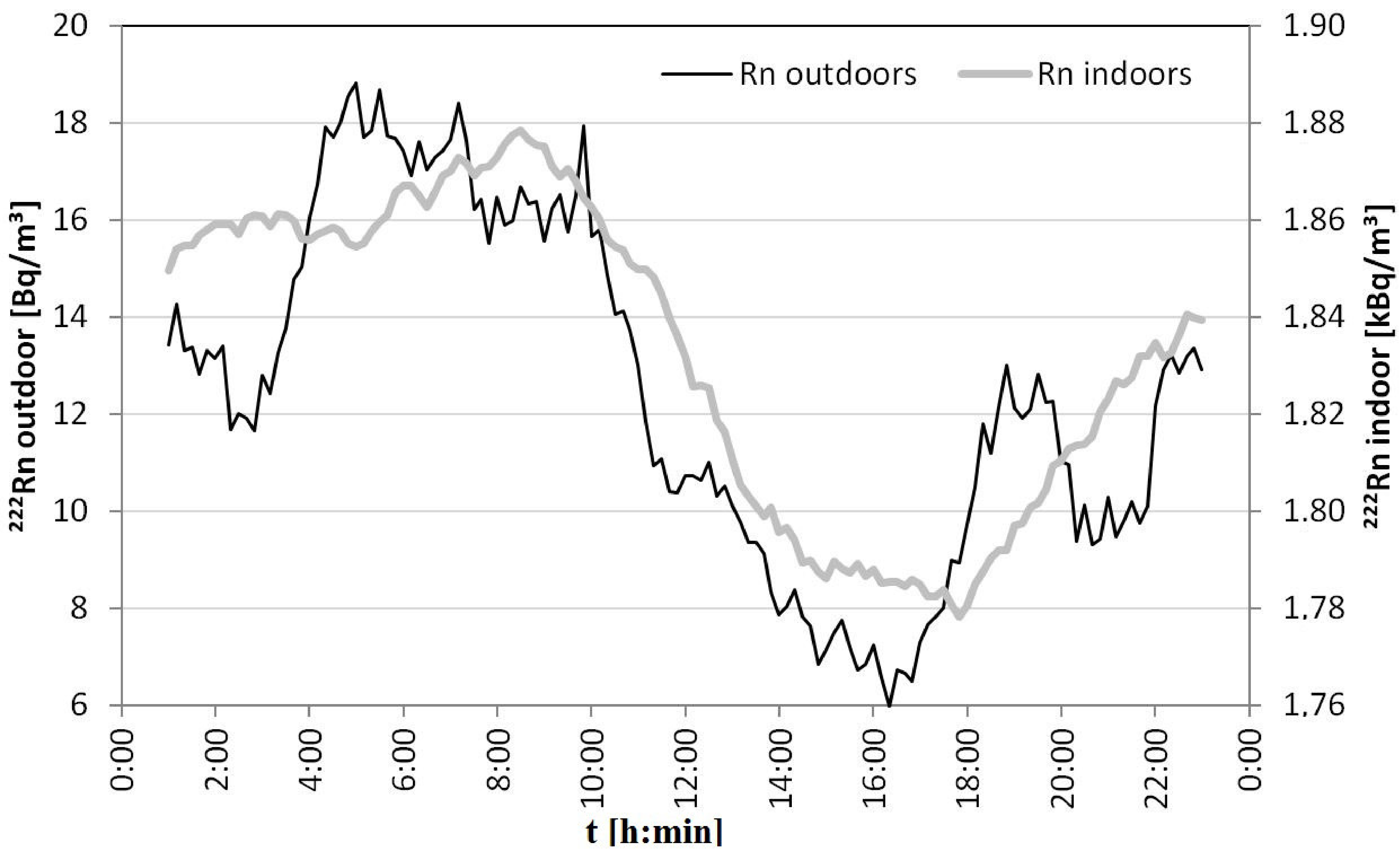
Rn outdoors
Rn indoors
222Rn outdoor [Bq/m3]
222Rn indoor [kBq/m3]
t [h:min]
20
18
16
14
12
10
8
6
1.90
1.88
1.86
1.84
1,82
1.80
1.78
1,76
0:00
2:00
4:00
6:00
8:00
10:00
12:00
14:00
16:00
18:00
20:00
22:00
0:00

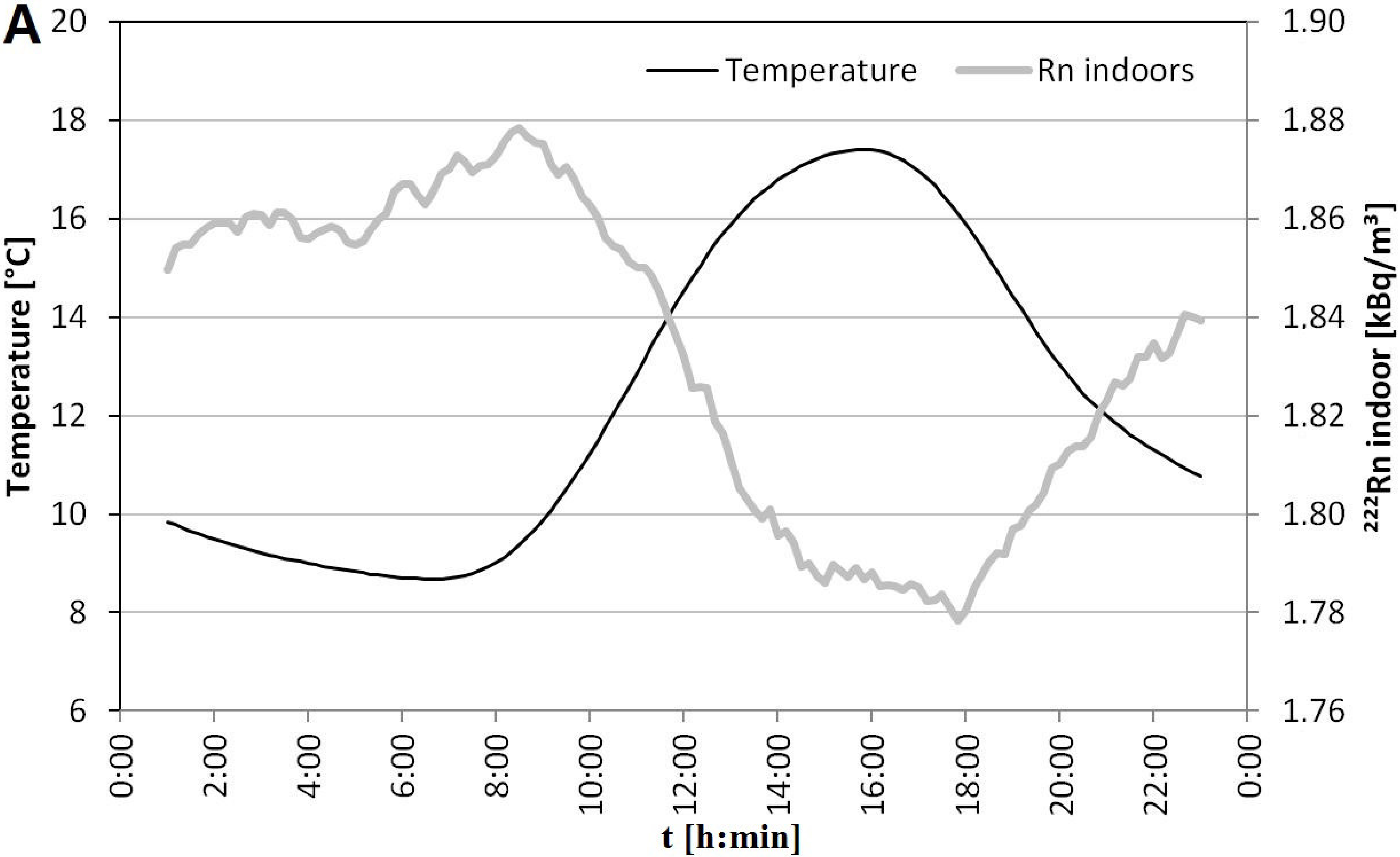
A
Temperature
Rn indoors
Temperature [°C]
222Rn indoor [kBq/m3]
t [h:min]
20
18
16
14
12
10
8
6
1.90
1.88
1.86
1.84
1.82
1.80
1.78
1.76
0:00
2:00
4:00
6:00
8:00
10:00
12:00
14:00
16:00
18:00
20:00
22:00
0:00

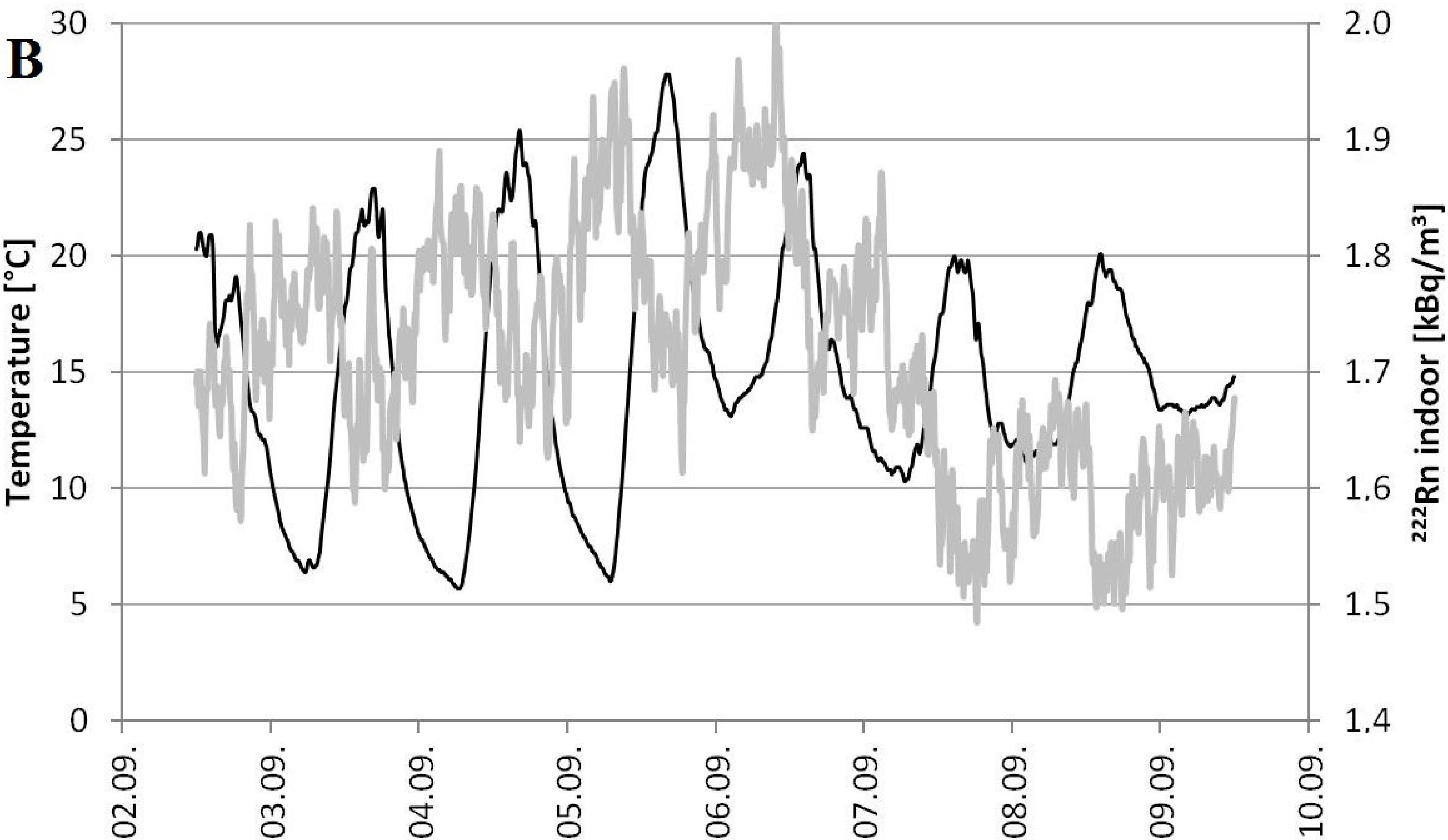

B
Temperature [°C]
30
25
20
15
10
5
0
222Rn indoor [kBq/m3]
2.0
1.9
1.8
1.7
1.6
1.5
1.4
02.09.
03.09.
04.09.
05.09.
06.09.
07.09.
08.09.
09.09.
10.09.

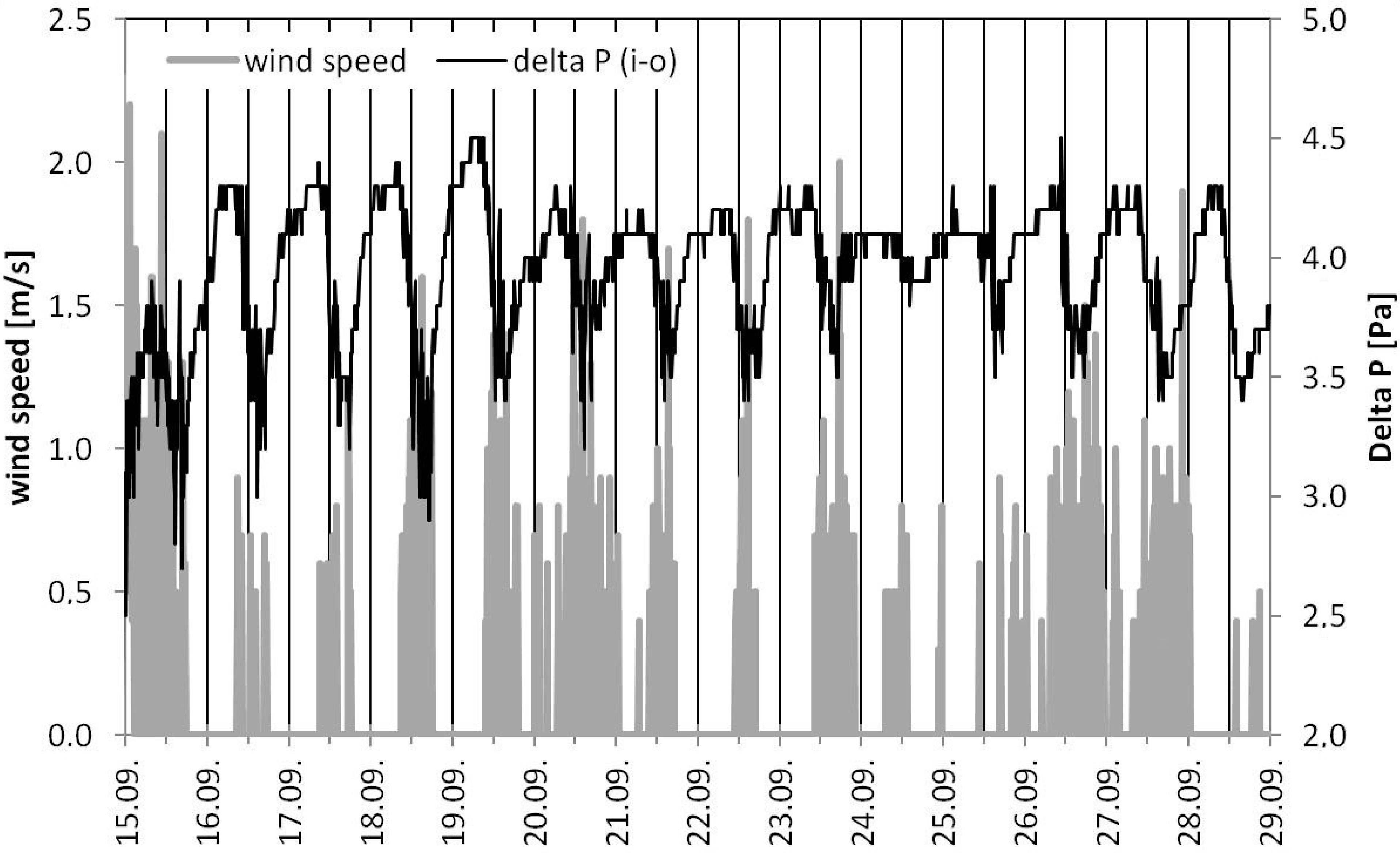

wind speed
delta P (i-o)
wind speed [m/s]
Delta P [Pa]
2.5
2.0
1.5
1.0
0.5
0.0
5.0
4.5
4.0
3.5
3.0
2.5
2.0
15.09.
16.09.
17.09.
18.09.
19.09.
20.09.
21.09.
22.09.
23.09.
24.09.
25.09.
26.09.
27.09.
28.09.
29.09.

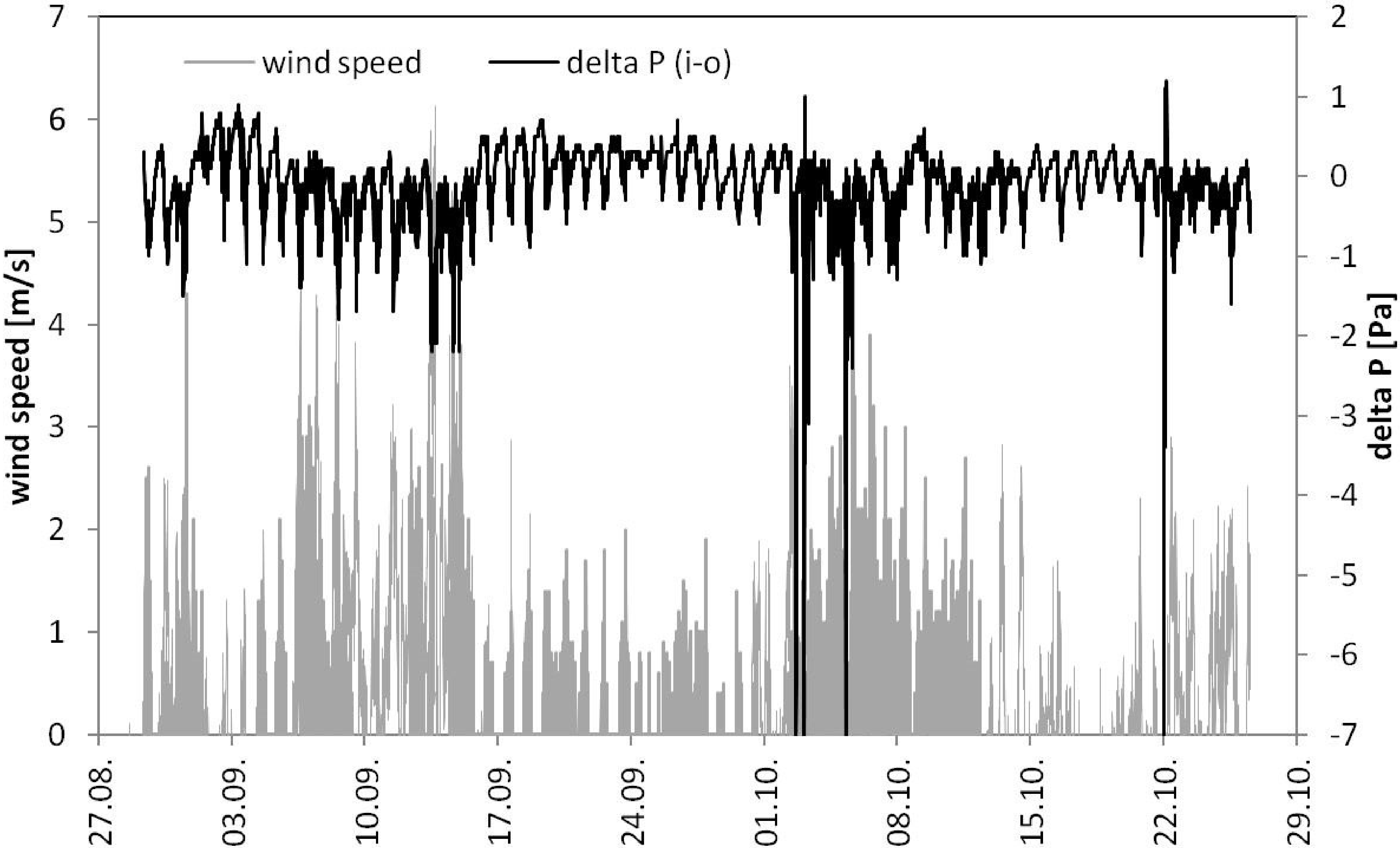

wind speed
delta P (i-o)
wind speed [m/s]
delta P [Pa]
7
6
5
4
3
2
1
0
2
1
0
-1
-2
-3
-4
-5
-6
-7
27.08.
03.09.
10.09.
17.09.
24.09.
01.10.
08.10.
15.10.
22.10.
29.10.

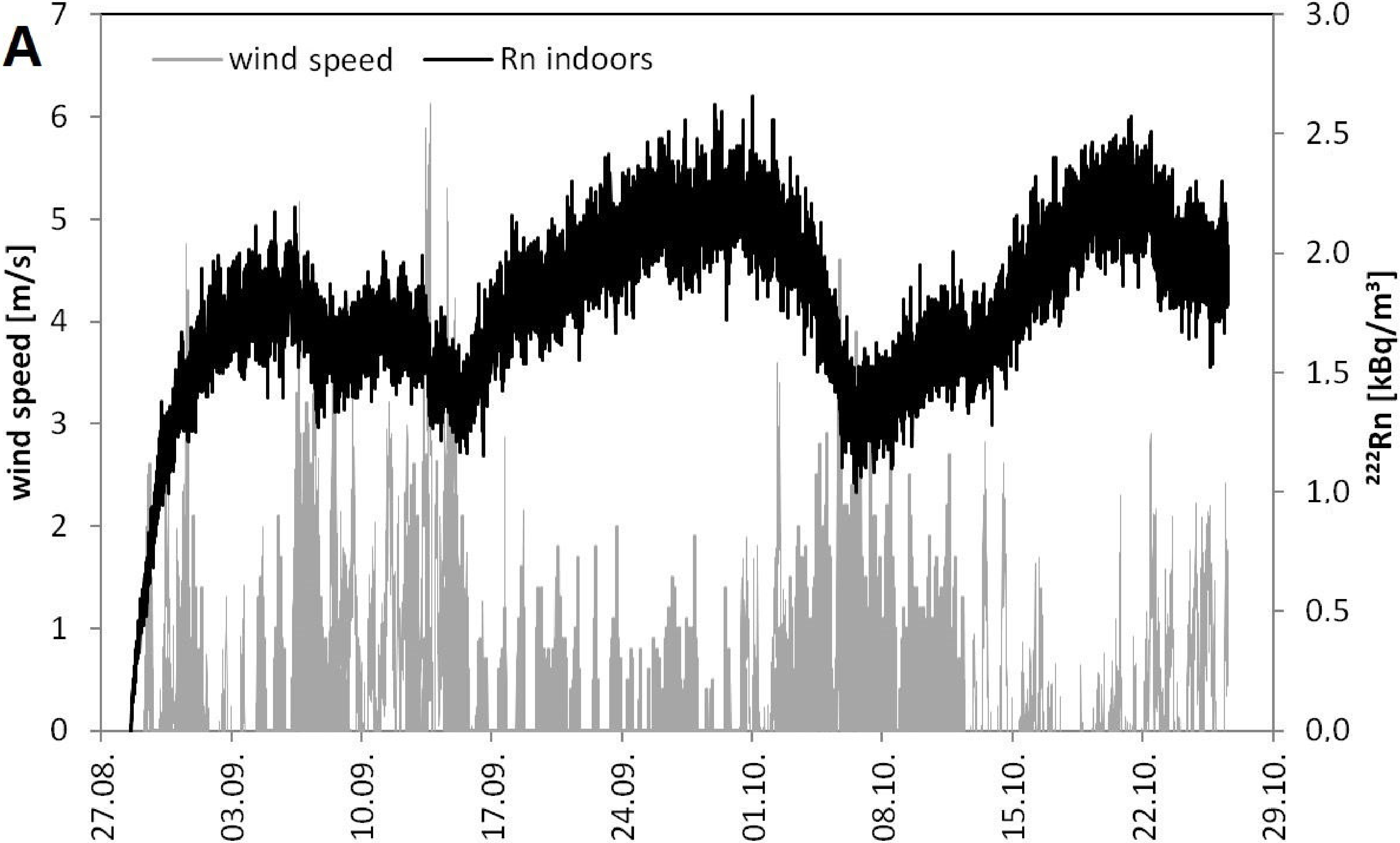

A
wind speed
Rn indoors
wind speed [m/s]
²²²Rn [kBq/m³]
0
1
2
3
4
5
6
7
0,0
0.5
1,0
1,5
2,0
2.5
3.0
27.08.
03.09.
10.09.
17.09.
24.09.
01.10.
08.10.
15.10.
22.10.
29.10.

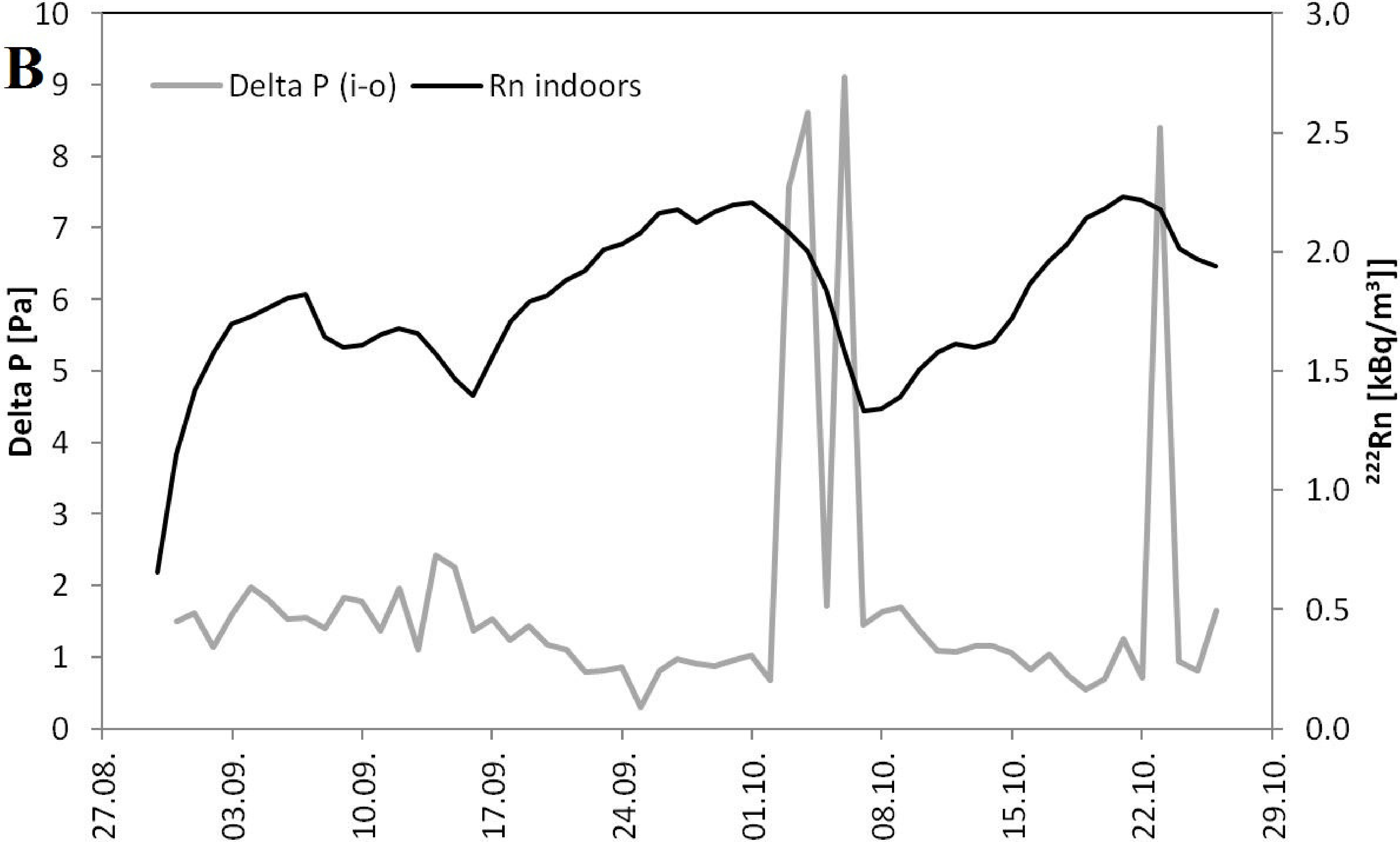

B
Delta P (i-o)
Rn indoors
Delta P [Pa]
^{222}Rn [kBq/m^3]]
10
9
8
7
6
5
4
3
2
1
0
3.0
2.5
2.0
1.5
1.0
0.5
0.0
27.08.
03.09.
10.09.
17.09.
24.09.
01.10.
08.10.
15.10.
22.10.
29.10.